A Novel Method for Detection and Classification of Covered Conductor Faults

Stanislav MISAK[1], *Michal KRATKY*[2], *Lukas PROKOP*[1]

[1]Centre ENET, VSB–Technical University of Ostrava, 17. listopadu 15, 708 33 Ostrava, Czech Republic
[2]Department of Computer Science, Faculty of Electrical Engineering and Computer Science, VSB–Technical University of Ostrava, 17. listopadu 15, 708 33 Ostrava, Czech Republic

stanislav.misak@vsb.cz, michal.kratky@vsb.cz, lukas.prokop@vsb.cz

DOI: 10.15598/aeee.v14i5.1733

Abstract. *Medium-Voltage (MV) overhead lines with Covered Conductors (CCs) are increasingly being used around the world primarily in forested or dissected terrain areas or in urban areas where it is not possible to utilize MV cable lines. The CC is specific in high operational reliability provided by the conductor core insulation compared to Aluminium-Conductor Steel-Reinforced (ACSR) overhead lines. The only disadvantage of the CC is rather the problematic detection of faults compared to the ACSR. In this work, we consider the following faults: the contact of a tree branch with a CC and the fall of a conductor on the ground. The standard protection relays are unable to detect the faults and so the faults pose a risk for individuals in the vicinity of the conductor as well as it compromises the overall safety and reliability of the MV distribution system. In this article, we continue with our previous work aimed at the method enabling detection of the faults and we introduce a method enabling a classification of the fault type. Such a classification is especially important for an operator of an MV distribution system to plan the optimal maintenance or repair the faulty conductors since the fall of a tree branch can be solved later whereas the breakdown of a conductor means an immediate action of the operator.*

Keywords

Covered conductor faults, fault type classification, medium-voltage, overhead lines with covered conductors, Partial Discharges, PD-pattern.

1. Introduction

The Covered Conductor (CC) have been primarily utilized for their high operation reliability guaranteed by the insulation compared to the ACSR. Consequently, the CC have been often used in forested or dissected terrain areas, in general, in all areas with extreme climatic conditions [1], [2] and [3]. Under these conditions, we can identify a high number of faults of the ACSR: the fall of a tree branch on the conductors, a phase-to-phase contact due to strong winds resulting in the phase-to-phase fault or, even, the breakdown of a conductor.

Therefore, the CC have been used for MV distribution lines for several decades. The major advantages of the conductor include:

- A high operational reliability since no short-circuit appears at the moment of the phase-to-phase contact.
- The individual phases can be located closer to one another and a demand on the protective zone of the overhead lines is lower compared to the ACSR.
- No immediate phase-to-phase contact appears when a tree branch falls on the conductors, and finally.
- The lines are not dangerous for birds sitting on the conductors.

The only disadvantage of using the CC is a difficult detection of faults when the conductor falls down on the ground. In this case, there is no single-phase-to-earth fault due to the insulation of the CC (let us note that it does not matter whether the conductor is broken). The standard protection relays work on the principle of an evaluation of the current or the voltage

at the point of the single-phase-to-earth fault. When the CC fault is not detected, the live CC lying on the ground can endanger individuals being close to the conductor or it can threat the reliability and safety of the distribution system. At the contact point, low-power capacitive current flows are generated by Partial Discharges (PDs). These PDs gradually degrade the CC insulation over time until the insulation system is locally destroyed. At this moment, the PDs are transformed into an arcing phase-to-ground fault and this fault is only detected by standard protection relays.

In this article, we continue with our previous work aimed at an electric voltage-based method enabling a detection of the CC faults [4] and [5] and we introduce a method enabling a classification of the fault type. Such a classification is especially important for an operator of an MV distribution system to plan the optimal maintenance or repair the faulty conductors since the contact of a tree branch can be solved later whereas the breakdown of a conductor means an immediate action of the operator.

In Section 2. , we categorize types of CC faults, in Section 3. , related works are described. In Section 4. , we introduce new indicators, and, in Section 5. , we put forward experiments in a climatic cabinet showing an ability of the indicators to classify the CC fault type. In Section 6. , we put forward an algorithm for the classification of the fault type. In Section 7. , the indicators are verified on a real 22 kV overhead line. In the last section, we conclude this article and we outline possibilities of our future work.

2. Problem Formulation - CC Fault Types

Following the previous section, the main problem of CC operating is a difficult detection of faults. The CC fault types can be divided into two basic categories differing from one another in terms of the time in which they are required to be eliminated.

Category I: It includes the most frequent faults where the climatic conditions in forested areas cause the contact of a tree branch with one or more phases of a CC overhead line or the fall of a tree on two or three phases of a CC overhead line. Category I faults represent the less dangerous incidents since a low degradation of the insulation system; these faults can be eliminated later [1] and [6].

Category II: It includes more dangerous faults which should be eliminated as soon as possible. In this case, a CC is exposed with an atmospheric overvoltage or an extensive degradation of the CC insulation leading to its breakdown and fall on the ground.

Both of the fault categories are characterized by PDs at the point where the CC insulation touches the ground, a tree branch, and so on. At this point, a non-homogeneous electric stray field appears and various types of PDs arise (inner, outer or surface [7], [8] and [9]); we talk about a PDs activity. It is important that these PDs types and corona discharges can be measured at the point of the fault [1], [6] and [10].

3. Research Background

The most widely discussed detection of the CC faults by PDs activity monitoring is a method using an analysis of the current signal flowing through the insulation system of a CC by means of a Rogowski coil [3], [11], [12], [13] and [14].

The electric current signal has two components, the carrier component with the frequency of the power supply (50 or 60 Hz) and the impulse component characterised by a PDs activity with a typical frequency range (e.g. 1–20 MHz). All the methods evaluate the impulse component. The main advantages of these methods are the good selectivity and sensitivity for CC faults of Category II. However, the good selectivity and sensitivity of these methods are required by the relative high cost of measuring apparatus. The most important parts of this measuring apparatus are the Rogowski coil and an A/D converter to impose the most demanding requirements in terms of (i) the accuracy of measuring the amplitude and phase in a wide frequency range, (ii) the resistance against external interferences, and (iii) the stability of a measurement for various climatic conditions. Evaluation of the actual state of the insulation system in the case of a fault of Category I is very difficult because of a small value of the impulse component [1], [3], [11] and [12]. Moreover, the small value of the impulse component is influenced by the load of CC overhead lines and also it has direct influence on the sensitivity of the impulse component evaluation.

In [4] and [5], we introduce a methodology for an evaluation of the PDs activity in the CC insulation system based on the electric voltage principle; we call it the CC fault detector. The main principles of the methodology are as follows: the electric stray field is measured using a sensor in the vicinity of the CC as a voltage signal (see Fig. 1). The sensor can be a single layer coil or a metal ring wrapped on the CC. The single layer coil with a turn-to-turn capacity forms one electrode of a compound dielectric medium, the second electrode is formed by the ground potential. The measured voltage signal is modified to the low level signal by a capacitive divider with a fixed ratio (CA in Fig. 1) whose primary side is connected with the terminal of the sensor. The voltage signal of the electric stray field clearly reveals the dominance of the carrier component

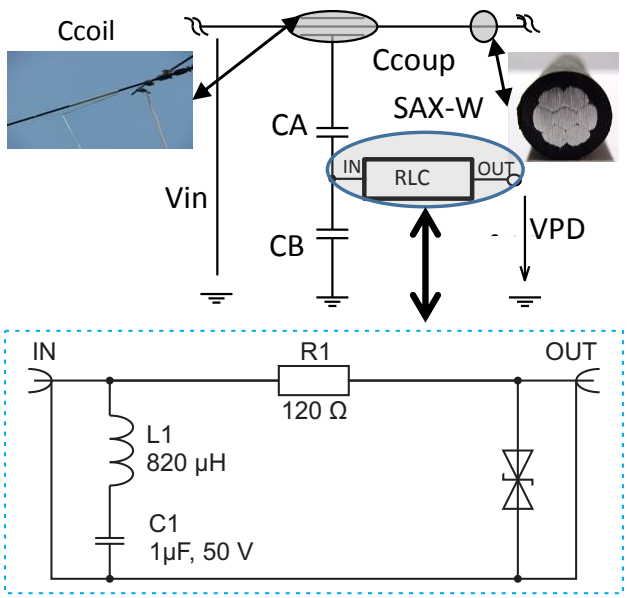

Fig. 1: Principal measurement diagram of the electric voltage-based method.

with the frequency of the power-supply unit, i.e. 50 Hz (the red line, the left axis in Fig. 2).

To evaluate the PDs activity, the impulse component is necessary (VPD in Fig. 1). The carrier component of the voltage signal has been therefore eliminated using the RC derivation block (the RLC block in Fig. 1). In this way, a time pattern of the impulse component is obtained. An example of the time pattern can be seen in Fig. 2 (the green line). We call the time pattern the PD-pattern in our article. An evaluation of a PD-pattern can provide an information about the actual state of the CC insulation system [4], [5], [15] and [16]. In [4] and [5] we also show that TRMS (True Root Mean Square) can be used for the evaluation of a PD-pattern.

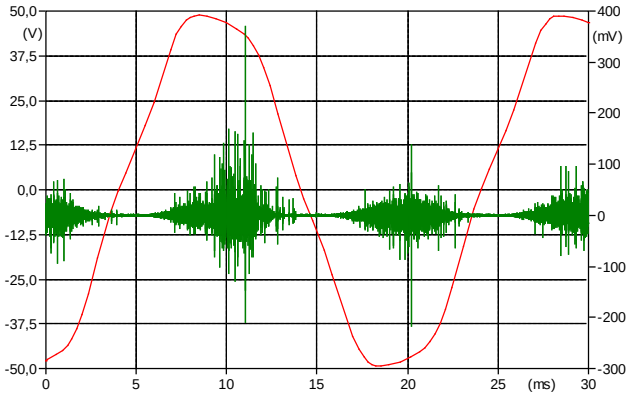

Fig. 2: Voltage signal of the electric stray field (the carrier component - the red line, the left axis; the impulse component - the green line, the right axis).

4. Indicator of CC Faults

The PD-pattern is the time pattern of the PDs activity which is specific for each CC fault type and climatic conditions at the point of a fault. Since a PD-pattern can provide an information about the actual state of the CC insulation system, in this paper, we utilize it for the classification.

The process of developing a fault indicator is divided into the following steps: 1) An analysis of PD-patterns for various types of CC faults and climatic conditions using the climatic cabinet in a framework of long-term testing (see Section 5.). 2) The development and implementation of the fault indicator and its integration in the CC fault detector (see Section 6.). 3) The verification of the fault indicator integrated in the CC fault detector in a real MV distribution system with the CC (see Section 7.).

We define three basic requirements on a fault indicator: (1) the low computational complexity, (2) the sensitivity for various CC fault types, (3) the capability to classify the CC fault type during a long-term time period. Let us describe these requirements in more details. (1): there is a need to find an indicator or indicators requiring the low computational performance in order not to increase the overall consumption of the fault detector. Moreover, the detector can be installed in inaccessible terrain and it can be supplied from, for example, a photovoltaic power station combined with a storage device. (2): the fault type has to be recognized during a short-term as well as 3): a long-term time period when a fault arises.

5. PD Pattern Analysis

As mentioned in the previous section, one aspect of the development of a fault indicator is an analysis of PD-patterns for various fault types and climatic conditions during a long-term measurement. For this purpose, an MV climatic cabinet was built, and three CC fault types of Categories I and II (see Tab. 1) in various climatic conditions (see Tab. 2) was simulated. During the tests, three different climatic conditions using the temperature and relative humidity were set.

The CC insulation system is naturally exposed with many other climatic influences [1] and [12], such as the atmospheric pressure or ultraviolet radiation, however these influences have not been simulated since it is difficult to keep the same conditions during the whole experiment. Similarly, it is not possible to simulate another fault type such as the fall of a tree on a CC.

Another factor important for a description of a PD-pattern is the time interval of a fault under various cli-

Tab. 1: CC faults simulated in the MV climatic cabinet.

Category	CC fault type	
I	The contact of a tree branch with the CC	
II	The fall of a CC on the ground	The soil
		The water

Tab. 2: Climatic conditions in the MV climatic cabinet.

Tempe-rature	Relative humidity	Abbr.	Type of day (The temperate zone)
(°C)	%		
−20	5	−20/5	Winter day
20	70	20/70	Spring or autumn day
60	15	60/15	Summer day(extremely sunny day)

matic conditions. Considering Indicator Requirement 3 (see Section 4.), the climatic cabinet enables us to test faults in a long period with a step size. For example, it enables us to test a fault for several days with the step size of 5 minutes. The following section puts forward the results of the tests for the selected fault types and climatic conditions. Since the PDs activity comes out as peeks in the impulse component of the voltage signal, we select the frequency of the PDs activity n (s^{-1}), i.e. the number of peaks per second, as a new indicator.

5.1. Category I - Contact of the Tree Branch with CC

The contact of a tree branch with a CC is one of the most frequent fault types. In Fig. 3, a PD-pattern of this fault is shown for the 20/70 climatic condition. In this figure, the PD-pattern is visualized as two lines; the red line represents the positive semi-period, and the green line represents the negative semi-period.

This fault type has two characteristic features. The first one is that peaks arise in both semi-periods of the PD-pattern (n is approximately 50 s^{-1}) and the

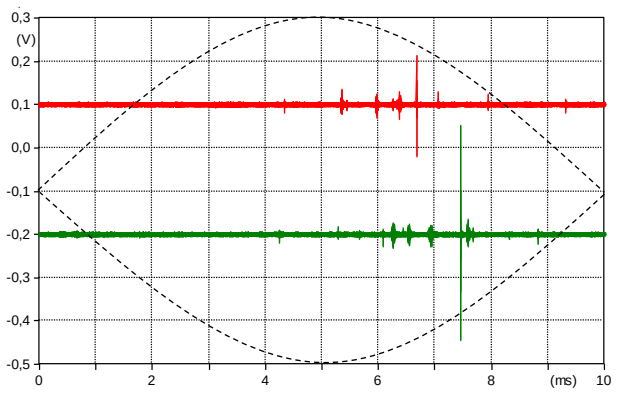

Fig. 3: PD-pattern - The contact of a tree branch with a CC, the climatic condition 20/70.

average amplitudes of the peaks are approximately the same in both semi-periods (70 mV). The second feature is the fact that the peaks occur when the supply voltage is going through the maximum values to 0.

In Fig. 4, the values of the indicator n during 75 hours after the fault arises can be seen. A long time interval of the contact of a tree branch with the CC means increased degradation of the insulation with the PDs activity. As a result, a diffusion of carbon particles into the contact point appears and the PDs activity is changed according to a climatic condition.

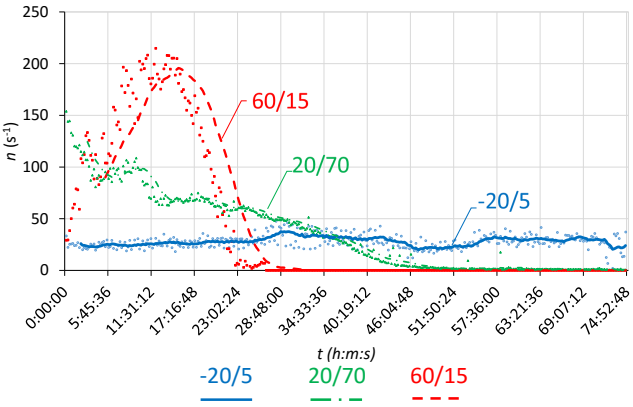

Fig. 4: Indicator n for the contact of a tree branch with CC.

In the case of the 20/70 climatic condition (see the green line in Fig. 4), a relatively intensive PDs activity (n = 150 s^{-1}) is caused by the high relative humidity. After some time (5 hours), a tree branch becomes dry at the contact point. As a result, the PDs activity is gradually reduced to n = 80 s^{-1}. Since the branch can have more contact points with the CC, the above mentioned process can appear again; however, the PDs activity is lower since electrical conductivity of the branch is lower.

When a time interval of the fault exceeds 46 hours, the branch becomes completely dry and the PDs activity is decreased to a negligible level.

In the second test, the 60/15 climatic condition (see the red line in Fig. 4), the PDs activity is low (n = 25 s^{-1}) when the fault appears due to the low relative humidity. Due to the high temperature, the insulation becomes soft and the number of contact points is increased. As a result, the PDs activity is gradually increased and it reaches the maximum n = 200 s^{-1} after 17 hours. After this point, the PDs activity rapidly decreases as the branch becomes dry; the PDs activity reaches a negligible level after 29 hours. In the third test, the −20/5 climatic condition (see the blue line in Fig. 4), the PDs activity is low (n = 25 s^{-1}) during the whole test since the low relative humidity.

Let us summarize the results; $n \in [25; 200]$ s^{-1} during 29 hours after the fault appears for all defined cli-

matic conditions and the frequency of peaks is approximately the same in both semi-periods.

5.2. Category II - Fall of CC on Ground - Soil

Although the fall of a CC on the ground does not belong to the most frequent faults, it is extremely dangerous. In this case, a CC falls on a solid surface, e.g. the soil or the clay, PDs occur in cavities of the conductor insulation. In Fig. 5, a PD-pattern of this fault is shown for the 20/70 climatic condition.

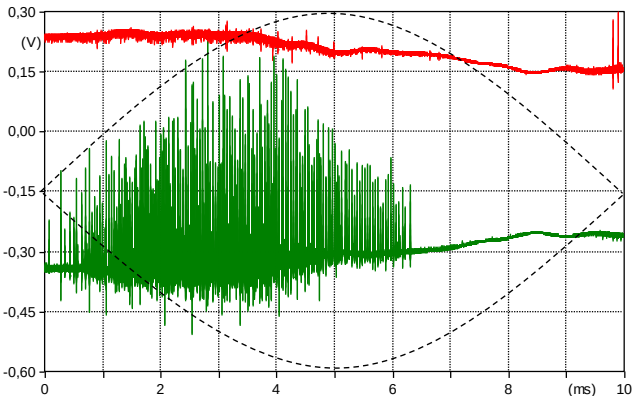

Fig. 5: PD-pattern - The fall of a CC on the ground - the soil, the climatic condition 20/70.

In this case, we distinguish three basic features. The first one, peaks mainly appear before the amplitudes in both semi-periods. The second one, n is up-to 13 000 s^{-1} compared to maximally $n = 200$ s^{-1} proposed for the previous fault type. The third one, there are less peaks with the low amplitude in the positive semi-period ($n = 150$ s^{-1}, the amplitudes is approx. 10 mV), on the other hand, there are more peaks with the high amplitude in the negative semi-period (n is up-to 10–100 higher, the amplitude is approx. 500 mV).

In the first test, the climatic condition 60/15 (see the red line in Fig. 6), a solid surface becomes dry and particles of isinglass create a glaze on the solid surface. It means a reduction of the number of contact points, and, consequently, the PDs activity is reduced ($n = 8\ 000$ s^{-1} when the fault appears); the PDs activity is decreased bellow a measurable level after 50 hours.

In the second test, the climatic condition −20/5 (see the blue line in Fig. 6), we can observe a similar situation as in the previous section in the case of the low relative humidity; the PDs activity is relatively low (compared to results of other climatic conditions) during the whole test because of low relative humidity. However, now $n = 1.500$ s^{-1} compared to $n = 25$ s^{-1} of the previous fault type.

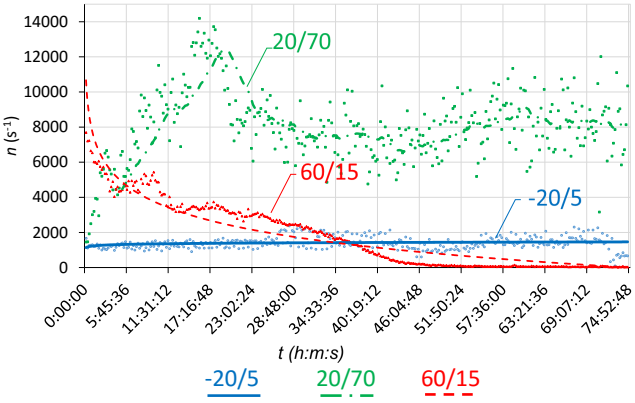

Fig. 6: Indicator n for the fall of a CC on the ground - the soil.

In the third test, the climatic condition 20/70 (see the green line in Fig. 6), the PDs activity gradually increases as the CC insulation degrades until a maximum is reached (approximately $n = 13\ 000$ s^{-1} after approx. 16 hours). After the maximum, the insulation becomes dry and particles of isinglass create a glaze on the solid surface and the PDs activity begins to decrease.

However, this process repeatedly appears since the electrical stability is exceeded in other parts of the insulation and we can observer other local maxima, e.g. after 60 hours in this case, and n therefore oscillates around 8 000 s^{-1}.

5.3. Category II - Fall of CC on Ground - Water

A PD-pattern of the fault type and the climatic condition 20/70 is shown in Fig. 7; the peaks appear close to the amplitudes of both semi-periods. We also see that the amplitudes of peaks are approx. 2 times higher in the positive semi-period, however, n is approx. 2 times higher in the negative semi-period.

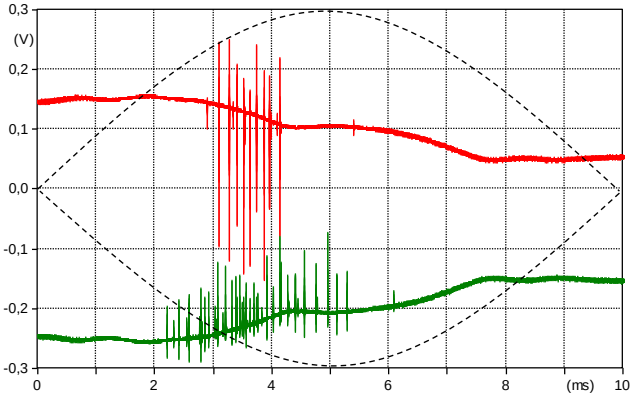

Fig. 7: PD-pattern - The fall of a CC on the ground - the water, the climatic condition 20/70.

In the first test, the climatic condition 20/70 (see the green line in Fig. 8), the long-term period of the measurement has no significant influence on the PDs activity; n oscillates around 300 s^{-1}.

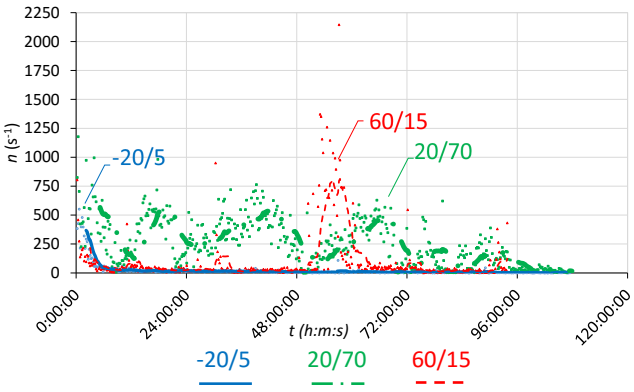

Fig. 8: Indicator n for the fall of a CC on the ground - the water.

In the second test, the climatic condition $-20/5$ (see the blue line in Fig. 8), the PDs activity is initially the same as in case of the first test ($n = 500$ s^{-1}). However, after a small time period (10 minutes), the PDs activity is minimal since the relative humidity is low. As a result, the insulation becomes dry and the number of contact points is reduced since the water surface is frozen.

In the third test, the climatic condition 60/15 (see the red line in Fig. 8), the PDs activity is initially low ($n = 50$ s^{-1}) since the number of contact points of a CC with the water surface is high (it is not necessary to reach so high energy to excite the PDs activity). After a number of hours, a condensation of water steam arises and the relative humidity is shortly increased. As a result, the PDs activity is also increased in this moment; $n = 1\ 300$ s^{-1}, after 60 hours.

6. Fault Indicator Development and Implementation

In the previous section, we can see that the frequency of peaks, i.e. the indicator n, characterizes well different fault types; however, there are some cases where it is necessary to compute the frequency of peaks in both semi-periods. Therefore, we define n_+ (s^{-1}) for the frequency of peaks in the positive semi-period and n_- (s^{-1}) for the frequency of peaks in the negative semi-period. We define the following indicator:

$$k = \frac{n_+}{n_-}(-). \tag{1}$$

Let us note that both indicators, n and k, satisfies three basic requirements proposed in Section 6.

In Tab. 3, the values of the indicators n and k for three fault types considered in a long-term period (after the 1st day, 3rd day, and 5th day) can be seen. We have to distinguish the fall of a CC on the ground (Category II) from other fault types (Category I) since it is the most dangerous fault and it has to be immediately repaired.

In Tab. 3, we can see that k is two orders of magnitude lower and n is one order of magnitude higher for the fall of a CC on the ground (the soil) compared to other fault types. As a result, if $k < 0.1$ it means this fault type occurs.

When we compare n for the contact of a tree branch with a CC and the fall of a CC on the ground, the water, n is often higher in the former case. Evidently, we need to utilize k to precisely distinguish both fault types; $k > 0.95$ for the contact and $k < 0.95$ for the fall. After the analysis, we can create a simple algorithm classifying the fault type (see Diagram on Fig. 9). To identify any fault type this algorithm utilizes a threshold, e.g. $n = 10$ s^{-1}.

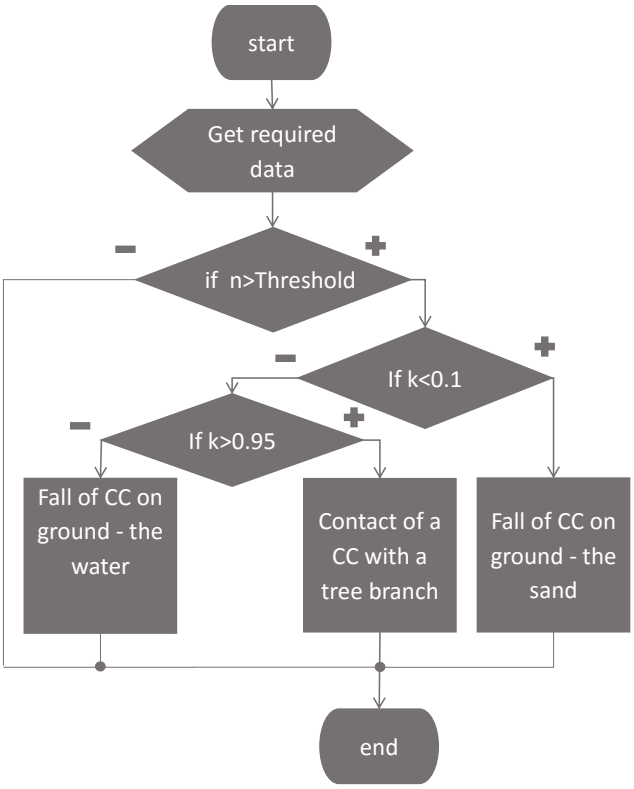

Fig. 9: Algorithm for a classification of the CC fault type.

In Tab. 3, we see that TRMS introduced in our previous work [4] and [5] is not appropriate for such a fault type classification. For example, we get the range [1.1, 8.9] for the fall of a CC on the ground (the

Tab. 3: Evaluation on indicators n and k for three fault types.

Temperature (°C)	Time period	The contact of a tree branch with a CC			The fall of a CC on the ground - the soil			The fall of a CC on the ground - the water		
		k (-)	n (s^{-1})	TRMS (V)	k (-)	n (s^{-1})	TRMS (V)	k (-)	n (s^{-1})	TRMS (V)
−20	1st day	1.23	52	0.10	0.03	1 670	1.46	0.75	158	3.57
	3rd day	1.00	54	0.15	0.04	2 009	1.53	0.67	28	0.79
	5th day	1.11	48	0.19	0.05	2 192	1.85	0.68	52	0.66
20	1st day	1.46	152	0.10	0.02	1 361	1.97	0.41	826	2.10
	3rd day	1.11	31	0.17	0.02	8 032	7.34	0.86	661	1.40
	5th day	1.00	18	0.12	0.04	8 992	8.48	0.83	17	0.41
60	1st day	1.00	15	0.16	0.07	4 664	8.85	0.81	77	4.62
	3rd day	1.11	13	0.08	0.08	329	2.10	0.52	88	1.17
	5th day	1.23	12	0.02	0.09	57	1.14	0.40	141	1.09

soil) and the range $[0.4, 4.7]$ for the fall of a CC on the ground (the water). These ranges are intersected and it means that we cannot distinguish these fault types using TRMS. Moreover, this value depends on the distance to the location of a fault.

7. Verification of Fault Detector

To verify the indicators n and k, we have installed the fault detector on a real 22 kV overhead line with the CC of the length 15 km. The overhead line is located in a forested area with a high number of faults; it is therefore appropriate for testing of the fault detector.

This detector was installed in September 2014 (see Fig. 10). PD-patterns together with the meteorological data have been measured one time per hour and they have been stored in a local disk of the fault detector. To analyse the data, we periodically download them and run a computation of the indicators n and k. To detect a fault, we set up the threshold of n to 10 s^{-1}. After the threshold is applied, we can classify the fault type using k.

Fig. 10: Fault detector and a detail of a sensor (a single layer coil with 75 turns).

Using the algorithm in Diagram in Fig. 9, we detect a fault after 2 months after the installation; the PD-pattern of the fault is shown in Fig. 11. The fault has been located 2.5 km from the detector. Since we measure and compute $n = 75$ s^{-1} and $k = 1.085$ (see

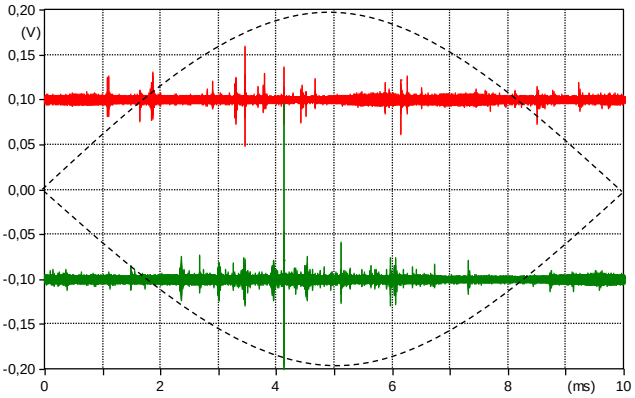

Fig. 11: PD-pattern of the fault.

Tab. 4), we distinguish the fault as the contact of a tree branch with a CC. The contact of a tree branch and the extent of damage are shown in Fig. 12. We measure the PDs activity during 48 hours after the fault appeared. This fault is repaired after 48 hours by an operator of the overhead line; we see that n is below the threshold. As a result, we verify the functionality of the fault detector in this way.

Tab. 4: Analysis of the PD-Pattern after the fault appears.

	2 hours	24 hours	48 hours
k	1.085	1.213	1.008
n	75	56	6

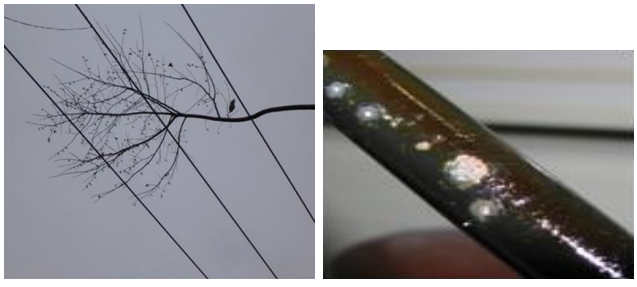

Fig. 12: Detected fault - the contact of a tree branch with a CC.

8. Conclusion

The main goal of this paper is to introduce new indicators for a classification of the CC fault type. We consider two categories of the fault type: Category I (the contact of a tree branch with a CC) and Category II (the fall of a CC on the ground). In our previous work, we utilize TRMS for a detection of a fault using an electric voltage-based method. In this paper, we show that it is not possible to use TRMS for the classification of the fault type, therefore, in this article we introduce two novel indicators n and k and we show that it is possible to use the indicators for the classification of the fault type using a simple algorithm. This algorithm has been designed after an analysis of experimental results in the climatic cabinet. It is important that the indicators fulfil three requirements defined in this paper. Compared to the other existing methods, electric current-based methods, the cost of our detector is lower and it enables the detection of a fault as well as the classification of the fault type. The fault detector utilizing the novel indicators has been installed on a real 22 kV overhead line with the CC and we have verified the fault detector in this way. In the near future, we will focus our research on development of new tools and methods for detecting long-distance faults and also we focus on improving sensitivity of developed method.

Acknowledgment

This paper is supported by the following projects: LO1404: Sustainable development of ENET Centre; SP2016/177, SP2016/128 (Students Grant Competition); LE13011: Creation of PROGRES 3 Consortium Office to Support Cross-Border Cooperation (CZ.1.07/2.3.00/20.0075) and the project of TACR TH01020426, Czech Republic.

References

[1] PAKONEN, P. *Detection of Incipient Tree Faults on High Voltage Covered Conductor Lines*. Tampere, 2007. Dissertation thesis. Tampere University of Technology.

[2] ZHANG, W., Z. HOU, H.-J. LI, C. LIU and N. MA. An improved technique for online PD detection on covered conductor lines. *IEEE Transactions on Power Delivery*. 2014, vol. 29, iss. 2, pp. 972–973. ISSN 0885-8977. DOI: 10.1109/TPWRD.2013.2288008.

[3] HASHMI, G., M. LEHTONEN and M. NORDMAN. Calibration of on-line partial discharge measuring system using rogowski coil in covered-conductor overhead distribution networks. *IET Science, Measurement & Technology*. 2011, vol. 5, iss. 1, pp. 5–13. ISSN 1751-8822. DOI: 10.1049/iet-smt.2009.0124.

[4] MISAK, S. and V. POKORNY. Testing of a covered conductor's fault detectors. *IEEE Transactions on Power Delivery*. 2015, vol. 30, iss. 3, pp. 1096–1103. ISSN 0885-8977. DOI: 10.1109/TPWRD.2014.2357072.

[5] HAMACEK, S. and S. MISAK. Detector of covered conductor fault. *Advances in Electrical and Electronic Engineering*. 2012, vol. 10, no. 1, pp. 7–12. ISSN 1804-3119. DOI: 10.15598/aeee.v10i1.567.

[6] AGARWAL, H., K. MUKHERJEE and P. BARNA. Partially and fully insulated conductor systems for low and medium voltage overhead distribution lines. In: *IEEE 1st International Conference on Condition Assessment Techniques in Electrical Systems (CATCON)*. Kolkata: IEEE, 2013, pp. 100–104. ISBN 978-1-4799-0082-4. DOI: 10.1109/CATCON.2013.6737537.

[7] BARTNIKAS, R. Partial discharges. Their mechanism, detection and measurement. *IEEE Transactions on Dielectrics and Electrical Insulation*. 2002, vol. 9, iss. 5, pp. 763–808. ISSN 1070-9878. DOI: 10.1109/TDEI.2002.1038663.

[8] DABBAK, S., H. ILLIAS, B. CHIN and A. TUNIO. Surface discharge characteristics on HDPE, LDPE and PP. *Applied Mechanics and Materials*. 2015, vol. 785, no. 5, pp. 383–387. ISSN 1662-7482. DOI: 10.4028/www.scientific.net/AMM.785.383.

[9] FORSSEN, C. and H. EDIN. Partial discharges in a cavity at variable applied frequency part 1: measurements. *IEEE Transactions on Dielectrics and Electrical Insulation*. 2008, vol. 15, iss. 6, pp. 1601–1609. ISSN 1070-9878. DOI: 10.1109/TDEI.2008.4712663.

[10] ACHILIDES, Z., E. KYRIAKIDES and G. GEORGHIOU. Partial discharge modelling: an improved capacitive model and associated transients along medium voltage distribution cables. *IEEE Transactions on Dielectrics and Electrical Insulation*. 2013, vol. 20, no. 3, pp. 770–781. ISSN 1070-9878. DOI: 10.1109/TDEI.2013.6518947.

[11] HASHMI, G. and M. LEHTONEN. Effects of rogowski coil and covered-conductor parameters on the performance of PD measurements in overhead distribution networks. *International Journal of Innovations in Energy Systems and Power*. 2010, vol. 4, no. 2, pp. 14–20. ISSN 0142-0615.

[12] HASHMI, G., M. LEHTONEN and M. NORDMAN. Modelling and experimental verification of on-line PD detection in MV covered-conductor overhead networks. *IEEE Transactions on Dielectrics and Electrical Insulation* 2010, vol. 17, iss. 1, pp. 167–180. ISSN 1070-9878. DOI: 10.1109/TDEI.2010.5412015.

[13] HEMMATI, E. and S. SHAHRTASH. Evaluation of unshielded rogowski coil for measuring partial discharge signals. In: *11th International Conference on Environment and Electrical Engineering (EEEIC)*. Venice: IEEE, 2012, pp. 434–439. ISBN 978-1-4577-1830-4. DOI: 10.1109/EEEIC.2012.6221417.

[14] SHAFIG, M., G. A. HUSSAIN, L. KUTT and M. LEHTONEN. Effect of geometrical parameters on high frequency performance of rogowski coil for partial discharge measurements. *Measurement*. 2013, vol. 49, iss. 1, pp. 126-137. ISSN 0263-2241. DOI: 10.1016/j.measurement.2013.11.048.

[15] CAVALLINI, A. and G. MONTANARI. Effect of supply voltage frequency on testing of insulation system. *IEEE Transactions on Dielectrics and Electrical Insulation*. 2006, vol. 13, iss. 1, pp. 111–121. ISSN 1070-9878. DOI: 10.1109/TDEI.2006.247849.

[16] STONE, G. C. Partial discharge diagnostics and electrical equipment insulation condition assessment. *IEEE Transactions on Dielectrics and Electrical Insulation*. 2005, vol. 12, iss. 5, pp. 891–904. ISSN 1070-9878. DOI: 10.1109/TDEI.2005.1522184.

About Authors

Stanislav MISAK was born in Slavicin in 1978. He received his Ing. and Ph.D. degrees in Electrical power engineering in 2003 and 2007, respectively, from the Department of Electrical Power Engineering, VSB–Technical University of Ostrava, Czech Republic, where he is currently an Associate Professor. Dr. Misak has published a number of articles in peer-reviewed journals and conference proceedings. He also holds a patent for a fault detector for medium-voltage lines. In 2012 he was appointed a delegate to the European Union Commission for the strategic management of renewable energy sources. He has been successful in obtaining a number of research contracts and grants from industry and government agencies for projects related to the areas of power systems and renewable energy integration. His current work includes the implementation of smart grid technologies using prediction models and bio-inspired methods and diagnostic of insulation systems.

Michal KRATKY was born in Olomouc in 1978. He is an associate professor at Department of Computer Science (`http://www.cs.vsb.cz/`), VSB–Technical University of Ostrava (`http://www.vsb.cz/`), from 2007. He received the Ph.D. degree in Computer Science in 2004. He has published more than 80 papers in the field of database systems (7 articles in journals with impact factor, e.g. VLDB Journal, Information Systems). He has been a head or a team member of 10 research projects (funded, e.g., by The Grant Agency of the Czech Republic, The Technology Agency of the Czech Republic). He has served as a member of 40 program and review committees of international conferences (e.g. DEXA 2007–2016, IDEAS 2015) and he has reviewed several journal and conference papers (Information Sciences, PODS 2015, DKE, IEEE Transactions on Information Theory and so on). There are 116 citations of his articles on SCOPUS, 390 on Google Scholar. He is the head of the Database Research Group (`http://db.cs.vsb.cz/`). He is a supervisor of 5 Ph.D. students, 2 students successfully defended their Ph.D. theses.

Lukas PROKOP was born in 1978 in Karvina. He received his Ing. degree in Electrical power engineering in 2002 from Brno University of Technology, Czech Republic, and his Ph.D. in Electrical power engineering in 2006 from VSB–Technical University of Ostrava, Czech Republic. In 2005 he joined the Department of Electrical and Computer Engineering at the VSB–Technical University of Ostrava, Czech Republic, where he is currently a research scientist. He is involved in a number of research contracts and grants from industry and government agencies, in the areas of power systems and renewable energy integration. His current work is focused on smart grid technologies, renewable energy sources, off-grid systems, power system reliability and power quality.